

Generation of Data Sets Simulating Different Kinds of Cameras in Virtual Environments

Yerai Berenguer, Luis Payá, Oscar Reinoso, Adrián Peidró and Luis M. Jiménez
Departamento de Ingeniería de Sistemas y Automática, Miguel Hernández University of Elche, Elche, Spain

Keywords: Data Set, Map Generation, Virtual Environment, Vision Systems, Image Description, Omnidirectional Images, Point Cloud Data.

Abstract: In this paper a platform to create different kinds of data sets from virtual environments is presented. These data sets contain some information about the visual appearance of the environment and the distance from some reference positions to all the objects. Robot localization and mapping using images are two active fields of research and new algorithms are continuously proposed. These algorithms have to be tested with several sets of images to validate them. This task can be made using actual images; however, sometimes when a change in the parameters of the vision system is needed to optimize the algorithms, this system must be replaced and new data sets must be captured. This supposes a high cost and slowing down the first stages of the development. The objective of this work is to develop a versatile tool that permits generating data sets to test efficiently mapping and localization algorithms with mobile robots. Another advantage of this platform is that the images can be generated from any position of the environment and with any rotation. Besides, the images generated have not noise; this is an advantage since it allows carrying out a preliminary test of the algorithms under ideal conditions. The virtual environment can be created easily and modified depending on the desired characteristics. At last, the platform permits carrying out another advanced tasks using the images and the virtual environment.

1 INTRODUCTION

Nowadays, there are many kinds of mobile robots that have to carry out different tasks autonomously in an unknown environment thus they must carry out two fundamental steps. On the one hand, the robot must create an internal representation of the environment (namely, a map) and on the other hand it must be able to use this map to estimate its current pose (position and orientation). The robot extracts information from the unknown environment using the different sensors that it may be equipped with. This information is compared with the map data to estimate the pose of the robot. Several kinds of sensors can be used with this aim, such as laser, touch or vision sensors.

Along the last years much research has been developed on robot mapping and localization using different types of sensors. A lot of these works use visual sensors since they permit many possible configurations and they provide the robot with very rich information from the environment that can be used in other high-level tasks (e.g. people detection, traffic lights identification, etc.) (Wang et al., 2016). Among them, some works focus on images with visual and

metrical information like RGB-d images. One example of this is showed in (Peasley and Birchfield, 2015) which uses this kind of information in mapping and tracking tasks.

The main contribution of the presented paper is the generation of image datasets simulating different kinds of cameras such as the omnidirectional systems that uses a hyperbolic mirror and the creation of datasets generating RGBd information, unlike other contributions that do not address this problems such as (Burbridge et al., 2006). It has a very useful purpose; the generation of data sets of images to design and improve algorithms that use any kind of visual information. To carry out this generation, a platform to create data sets of images changing the type of camera and all the vision system parameters has been developed. These systems can be simple cameras, stereo cameras, panoramic cameras or catadioptric vision systems, which provide the robot with omnidirectional scenes from the environment (Winters et al., 2000). We can find many previous works that use omnidirectional images in mapping and localization tasks (Valiente et al., 2014) present a comparison between two different visual SLAM methods us-

ing omnidirectional images and (Maohai et al., 2013) propose a topological navigation system using omnidirectional vision. This catadioptric virtual system is composed of a camera pointing to a hyperbolic mirror.

We must also take into account the fact that, nowadays, UAVs (Unmanned Aerial Vehicles) have become very popular and versatile platforms that can do several tasks. Some researchers have faced previously the problem of localization with this kind of platform, such as (Mondragon et al., 2010).

Traditionally, the developments in mobile robotics mapping and localization using visual sensors are based on the extraction and description of some landmarks from the scenes, such as SIFT (Scale-Invariant Feature Transform) (Lowe, 1999) and SURF (Speeded-Up Robust Features) (Bay et al., 2006) descriptors. More recently some works propose using the global information of the images to create the descriptors. These techniques have demonstrated to be a good option to solve the localization and navigation problems. (Payá et al., 2010) and (Wu et al., 2014) propose two examples of this.

In all these works, it is necessary to have a complete set of scenes to validate the visual mapping and localization algorithms. Traditionally, the robotic platform is equipped with a vision system and the robot is teleoperated through the environment to map while the robot captures the set of images from several points of view.

This method presents some disadvantages. For example, the process to obtain the sets is slow and expensive. Also, it is quite difficult to know with accuracy the coordinates of the positions where each image is acquired. At last, to test the effect that some changes in the geometry of the vision system may have on the algorithm, it is necessary to capture new sets of scenes for each new geometry.

In this work we implement a platform to create visual information simulating different visual systems mounted on the robot. This platform is useful to create sets of scenes without any additional cost. These sets can be used to validate any new mapping and localization algorithm that uses visual information. These maps can be created using different number of images and different map typologies, such as trajectory or grid maps. Furthermore, these maps can contain as many images as required. The platform also permits changing the geometry and configuration of the vision system, apart from other map parameters.

Besides, to test the localization algorithms in a previously built map, it is possible to obtain test images from any map position simulating any rotation or orientation of the robotic platform in the space (6

degrees of freedom). Another advantage of this platform is that the images created have not any noise or imperfection because they are captured from a virtual environment defined previously. It permits testing the different algorithms under ideal conditions, what can be useful in the initial stages of the design and tuning of a new algorithm. Furthermore, the noise or occlusions can be added afterwards to test robustness of the algorithms once they have been tuned with ideal images.

This way, we expect that the use of this platform saves time and money during the development of new mapping and localization algorithms. Thanks to it, the initial experiments can be carried out quickly, in a variety of environments and with accuracy.

The remainder of this paper is structured as follows. Section 2 introduces the vision systems we use to create the images: the simple camera, the stereo camera, the panoramic camera and the omnidirectional vision system. Section 3 presents the algorithm we have designed to simulate the vision systems. Section 4 describes some additional options the platform offers. Section 5 presents the experiments and results. At last section 6 outlines the conclusions.

2 SIMULATING VISION SYSTEMS

Nowadays, there are several types of visual sensors. The platform presented in this work simulates some of them, in particular, simple cameras, stereo cameras, panoramic cameras and catadioptric vision systems.

The basis of the simulation of all these systems is mainly based on the beam trajectory from the objects in the environment to the camera focus. All of these vision systems are very commonly used in uncountable number of works. The catadioptric system presents the most complex image formation process. For this reason, the simulation algorithm is explained using this kind of vision system as a basis. The rest of vision systems are simulated using the same concepts.

2.1 Omnidirectional Vision System

The omnidirectional images (Figure 1(a)) are created using a catadioptric vision system consisting of a camera mounted on the robot and pointing usually to a hyperbolic mirror (Figure 1(b)). The optical axis of the camera and the axis of the mirror are aligned. The camera captures the image reflected on the hyperbolic mirror forming the omnidirectional image. The Figure 2 shows how a point in the space is reflected on the mirror \vec{P} and subsequently projected

to the image plane, p . (i, j) is the reference system of the image plane and (x_c, y_c, z_c) is the world reference system. The figure shows some of the most relevant parameters of the hyperbolic mirror and the camera.

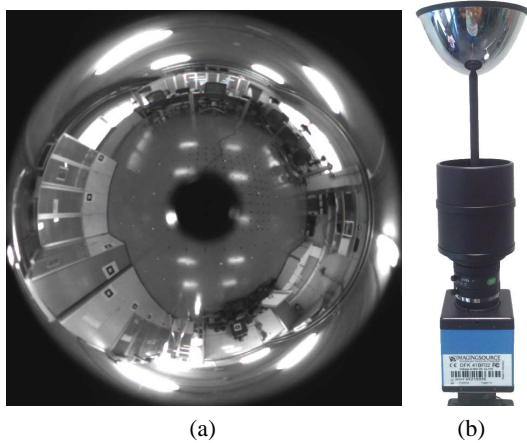


Figure 1: (a) Actual omnidirectional image. (b) Actual omnidirectional vision system.

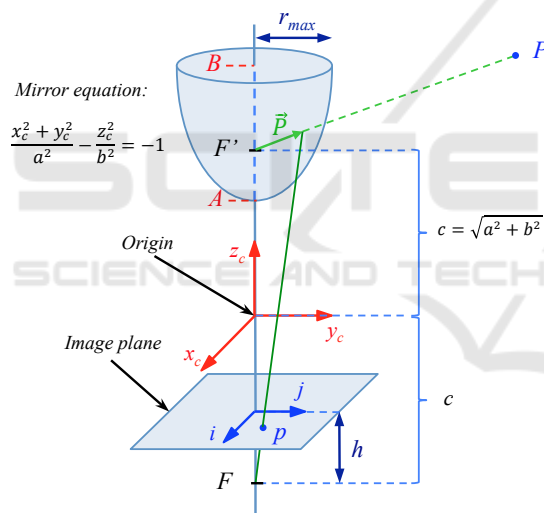


Figure 2: Catadioptric system used to capture the synthetic omnidirectional images, using a hyperbolic mirror.

The basis of this system is mainly based on the beam trajectory from the objects in the environment to the camera focus (F). Firstly, the beam leaves from the objects and it arrives to the hyperbolic mirror. Finally, the beam reflects on the mirror and goes towards the camera focus (F), appearing on the image plane.

The Equation 1 defines the hyperbolic mirror. This mirror is symmetric and its dimensions are defined by a and b . These variables also define the distance between the focus of the hyperbolic mirror and the origin of the world coordinate system, c (Equation 2).

$$\frac{x_c^2 + y_c^2}{a^2} - \frac{z_c^2}{b^2} = -1 \quad (1)$$

$$c = \sqrt{a^2 + b^2} \quad (2)$$

The hyperbolic mirrors are widely used to create omnidirectional images thanks to their properties (Zivkovic and Booij, 2006). However, there are many other kinds of vision systems that provide omnidirectional images, such as parabolic mirrors, spherical mirrors or conic mirrors (Nene and Nayar, 1998) and even polar arrays of cameras (Perazzi et al., 2015).

Equation 3 defines the equation of parabolic mirrors and Equation 4 defines the equation of spherical mirrors.

$$\frac{z_c}{c} = \frac{x_c^2}{a^2} + \frac{y_c^2}{b^2} \quad (3)$$

$$(x_c - x_0)^2 + (y_c - y_0)^2 + (z_c - z_0)^2 = r^2 \quad (4)$$

where (x_0, y_0, z_0) are the coordinates origin of the sphere with respect to the reference system (x_c, y_c, z_c) ; a, b, c define the geometry of the parabolic mirror and r is the sphere radius.

Starting from an omnidirectional image it is possible to obtain a panoramic version using a simple program to transform the polar coordinates of the omnidirectional image into the cartesian coordinates of the panoramic image. The Figure 3 shows the panoramic image obtained from the omnidirectional image showed in Figure 1(a). The platform is also very useful to obtain other different projections such as orthographic views, cylindrical and unit sphere projections. Some mapping and localization algorithms make use of such information (Amorós et al., 2014).



Figure 3: Panoramic image obtained from the omnidirectional image of Figure 1(a).

3 SIMULATION ALGORITHM

In this work, the vision systems are modeled by an algorithm with the purpose of creating images from a virtual environment. This program is based on the beams trajectory and the intersections between planes and straight lines.

To generate an image, it is necessary first to create a virtual environment. This environment has to

be defined in such a way that the intersection between the beams and the objects within this environment can be simulated efficiently. We have defined these objects as clusters of faces and each of these faces is contained in a different plane. As an example, six faces in six different planes define a cube. From this standpoint, the virtual environment is formed by a set of faces in the space defining objects with different shapes. The Figure 4 shows the elements that form a parallelepiped using these faces; the parallelepiped is defined by l_1, l_2, l_3 , its position in the environment and the color of each face.

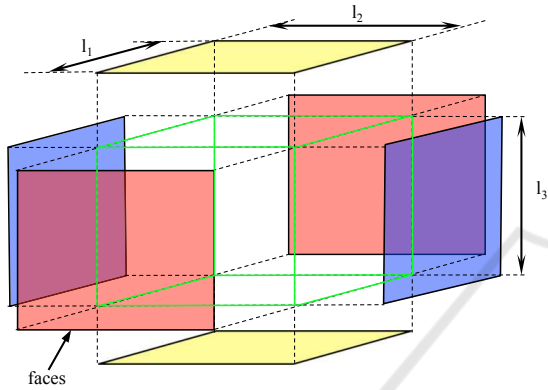


Figure 4: Faces of an object in a virtual environment.

Once all the objects have been generated, the algorithm creates the images by calculating each beam trajectory in the system.

Considering that the most complex vision system is the catadioptric system, the algorithm is explained using the omnidirectional vision as a basis for the explanation. The other systems have been simulated using the same concepts.

Firstly, the image plane is defined choosing the resolution of the omnidirectional image ($k_x \times k_y$) and the distance h in Figure 2 (distance between the image plane and the focus of the camera).

Secondly, the vector $\vec{F}p_{ij}$ is calculated from the focus of the camera F to each pixel in the $image(i, j)$ per each pixel of the image plane (Equation 5). p_{ij} is the pixel selected to trace the beam. The Figure 5 shows the image plane and the beam trajectory per each pixel p_{ij} .

$$\vec{F}p_{ij} = \vec{p}_{ij} - \vec{F} \quad (5)$$

where \vec{p}_{ij} and \vec{F} are the vectors whose components are the coordinates of p_{ij} and F respectively, with respect to the world reference system $\{x_c, y_c, z_c\}$.

Thirdly, the straight line $r1_{ij}$ defined by the vector $\vec{F}p_{ij}$ and the point F (as a point of this line) is used to calculate the intersection point (Q_{ij}) between $r1_{ij}$ and the hyperbolic mirror (Equation 1).

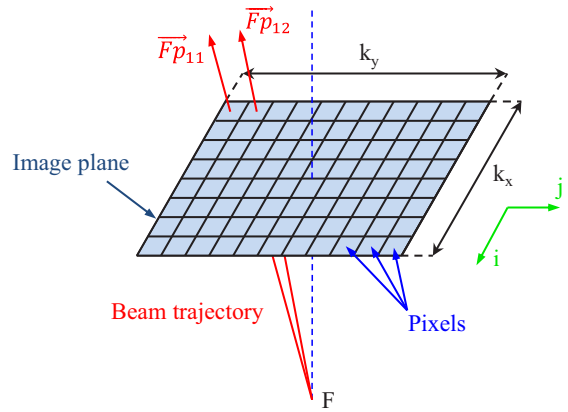


Figure 5: Beam trajectories for each pixel in the image plane.

Fourthly, this point (Q_{ij}) is used to calculate the vector \vec{P}_{ij} by means of this equation:

$$\vec{P}_{ij} = \vec{Q}_{ij} - \vec{F}' \quad (6)$$

where \vec{Q}_{ij} and \vec{F}' are the vectors whose components are the coordinates of Q_{ij} and F' respectively, with respect to the reference system $\{x_c, y_c, z_c\}$. F' is the focus of the hyperbolic mirror (Figure 2).

Finally, the straight line $r2_{ij}$ defined by the vector \vec{P}_{ij} and the point F' is used to calculate the intersection point (P) between them and any object in the environment. When $r2_{ij}$ intersects with a face of an object, the pixel of the image plane used in Equation 5 takes the color value of that face of the object. $r2_{ij}$ may intersect with several faces, but only the first intersection is considered (this is what happens in a real situation).

Therefore, this process creates a cluster of vectors composed of all of the vectors \vec{P}_{ij} , one per each pixel of the plane image, and a point (F'). The intersections with the objects in the environment are calculated using the lines defined by these vectors and the point (F').

To simulate the translation of the robot it is only necessary translate the point (F'). The cluster of vectors is not modified. The change in robot elevation is simulated using a translation in the z axis. The following equation shows the translation of the point F' :

$$\vec{F}'_T = \vec{F}' + \vec{T} \quad (7)$$

where \vec{F}'_T is the vector whose components are the coordinates of F'_T , with respect to the reference system $\{x_c, y_c, z_c\}$. F'_T is the point F' translated and T is the translation vector.

At last, to take into consideration that the robot may have different orientations in the space, it is necessary to use one or more rotation matrices to transform each vector \vec{P} :

$$R_x(\theta_x) = \begin{bmatrix} 1 & 0 & 0 \\ 0 & \cos \theta_x & -\sin \theta_x \\ 0 & \sin \theta_x & \cos \theta_x \end{bmatrix} \quad (8)$$

$$R_y(\theta_y) = \begin{bmatrix} \cos \theta_y & 0 & \sin \theta_y \\ 0 & 1 & 0 \\ -\sin \theta_y & 0 & \cos \theta_y \end{bmatrix} \quad (9)$$

$$R_z(\theta_z) = \begin{bmatrix} \cos \theta_z & -\sin \theta_z & 0 \\ \sin \theta_z & \cos \theta_z & 0 \\ 0 & 0 & 1 \end{bmatrix} \quad (10)$$

$$R_{total} = R_x(\theta_x) \cdot R_y(\theta_y) \cdot R_z(\theta_z) \quad (11)$$

$$\vec{PR}_i = R_{total} \cdot \vec{P}_i \quad (12)$$

where R_x , R_y and R_z are the rotation matrix with respect to each axis, R_{total} is the resulting rotation matrix and \vec{PR}_i is the vector \vec{P} rotated.

The scheme of the generation process of the omnidirectional images is defined in Code 1.

Code 1: Simulation pseudocode.

```

1 for i=1:1:px
3   for j=1:1:py
5     Choose the point p(i,j) from the
       image plane
7     Calculation of v_Fp(i,j) =p(i,j)-F
9     r1 is defined by v_Fp and F
11    pi(i,j)=intersection between r1 and
       the hyperbolic mirror
13    Calculation of v_P(i,j)=Q(i,j)-F'
15    r2 is defined by v_P and F'
17    P=first intersection point between
       the line r2 and an object in the
       virtual environment
19    image(i,j)=color of the object in the
       point P
21 end
23 end
    
```

4 ADDITIONAL IMAGE CAPTURE OPTIONS AND DESCRIPTION

The main objective of this work is to present a platform to create images from a virtual environment as presented in the previous section. Besides this function, the platform can carry out another advanced tasks using the foundations presented in Section 3.

Since this platform has been designed to test localization and mapping algorithms we include some of the most used image description methods. We have included both local landmark extraction methods and global appearance methods.

On the one hand, the platform permits extracting and describing both the SIFT (Scale-Invariant Feature Transform) (Lowe, 1999) or SURF (Speeded-Up Robust Features) (Bay et al., 2006) features from each virtual omnidirectional image to carry out experiments using this kind of descriptors. All the parameters are tunable.

On the other hand, several global appearance descriptors can also be calculated using the platform. Some examples are the Radon transform (Radon, 1917; Berenguer et al., 2015), the Fourier Signature (FS), Principal Components Analysis (PCA), Histogram of Oriented Gradients (HOG) and *gist* descriptor. Many of these descriptors are used in the work of (Payá et al., 2014). And also, the user can configure all the parameters.

The creation of each environment is very easy through command lines. It is possible to create any new object defining its shape, position, orientation and size. The virtual environments can be defined indoors or outdoors.

This is very useful to test the localization algorithms under realistic conditions. Usually, the map images are captured on a specific time of day but the localization must be carried out in different moments. It implies different lighting conditions and also other changes in visual information, such as occlusions in scenes due to the presence of persons or other mobile objects around the robot.

Taking these facts into account, the platform has also other configurable options to generate the images such as adding light points, noise and occlusions (adding objects in the virtual environment). It is also possible to change the color of each object in the virtual environment.

The omnidirectional images can also be transformed in different projections (such as orthographic views, cylindrical and unit sphere projections) using the platform presented. It is an interesting characteristic because there are many works that use panoramic

images and other projections in localization tasks (Payá et al., 2014).

At last, nowadays, some researches make use of point cloud data in localization tasks, such as (Andreasson and Lilienthal, 2010). An additional option has been added to the platform to generate the point cloud data of the virtual environment. This process consists in saving all P points (intersection point between each line r_2 and the objects in the virtual environment). This point cloud data saves the coordinates x , y and z of each point P and the color of the object in this point and emulates the information captured by an RGB-d camera. The Figure 6 shows a point cloud data of a sample virtual environment captured using a simple virtual camera.

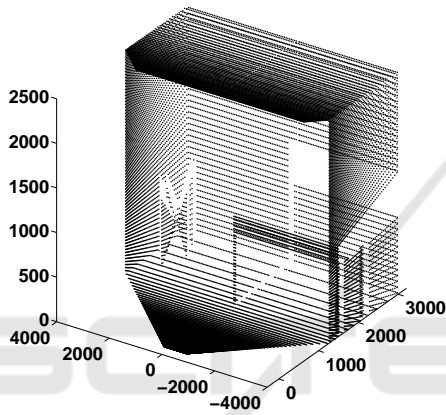


Figure 6: Point cloud data of a sample virtual environment.

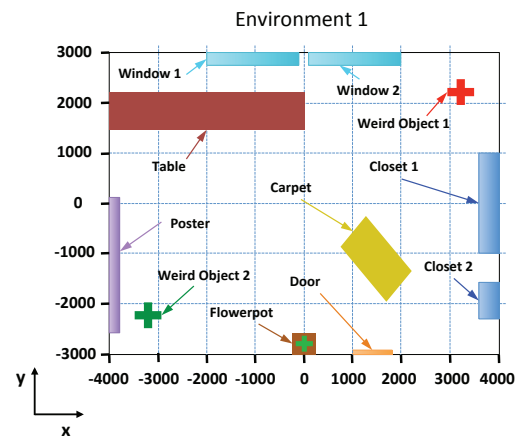
The presented platform uses a simple user interface which uses an object library to create the virtual environment. Also, this interface permits creating a path to generate images along it.

5 EXPERIMENTS

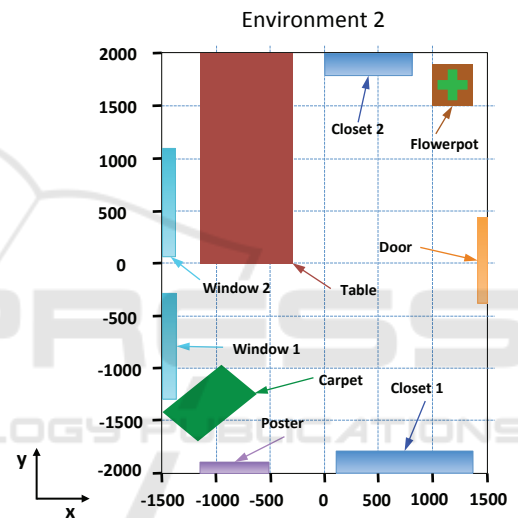
In order to check the performance of the proposed method, we have created two virtual environments which represent two different rooms. In these environments it is possible to create an image using different types of vision systems from any position and orientation. The Figure 7 shows a bird eye's view of both environments.

Different sample images have been taken using several kinds of visual systems. The figure 8 shows three different kinds of images taken using a single camera, a panoramic camera and a stereo camera.

The resolution of the images can be configured freely. To generate omnidirectional images, we have chosen 250×250 pixels to carry out the experiments. The parameters used in the mirror equation (Equation



(a)



(b)

Figure 7: (a) Bird eye's view of the environment 1. (b) Bird eye's view of the environment 2. (Dimensions in millimeters).

1) can also be configured, in this experiment we have chosen $a = 40$ and $b = 160$.

Several sets of images have been captured in each environment, considering changes in robot elevation, translation, rotation and inclination before capturing each new image. The figure 9 shows the coordinates of the mirror focus F' , the rotation in each axis, and the generated images.

As mentioned previously in Section 4, the platform can also transform these omnidirectional images in orthographic views, cylindrical and unit sphere projections. The Figure 10 shows an example of the panoramic transformation of an omnidirectional image from the environment 1.

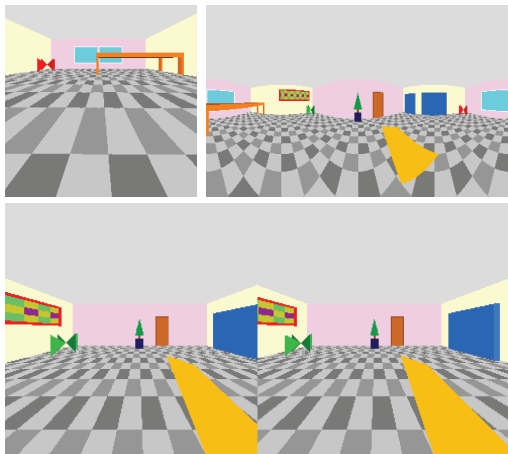


Figure 8: Different kinds of visual systems. Top left, single camera. Top right, panoramic camera. Bottom, stereo camera.

6 CONCLUSIONS

In this work a platform to create different kinds of images using virtual environments has been presented. This method is mainly based on the beams trajectory and the intersections between planes and straight lines. Furthermore, it can create images from any position of the environment and with any robot orientation.

The platform can also extract SIFT and SURF features of each image, create global appearance descriptors (Radon, FS, PCA and HOG), add changes in the environment (light points, noise, occlusions and colors). Also it is possible to generate images using different kinds of visual sensors such as single cameras, panoramic cameras, stereo cameras and catadioptric systems, and, at last, the platform can save the point cloud data of the environment.

The experiments included in this paper generate our own image database created synthetically from two different environments. The results demonstrate that the method is able to create sets of omnidirectional images with flexibility and efficiency.

We expect this platform constitutes an alternative to generate easy, quickly and with flexibility image sets to test and tune any new visual mapping and localization algorithm. This may help to accelerate the initial stages of the algorithm design and to find more quickly the optimal value for the parameters of the visual system, images and the descriptors.

The results of this work encourage us to continue this research line. It will be interesting to improve this platform to add more types of changes in the environment such as shadows. Also, this method will permit

	Environment 1	Environment 2
$F'(0,0,0)$ $\theta_x = 0 \text{ deg}$ $\theta_y = 0 \text{ deg}$ $\theta_z = 0 \text{ deg}$		
$F'(0,0,40)$ $\theta_x = 0 \text{ deg}$ $\theta_y = 0 \text{ deg}$ $\theta_z = 0 \text{ deg}$		
$F'(150,0,40)$ $\theta_x = 0 \text{ deg}$ $\theta_y = 0 \text{ deg}$ $\theta_z = 0 \text{ deg}$		
$F'(150,0,40)$ $\theta_x = 0 \text{ deg}$ $\theta_y = 0 \text{ deg}$ $\theta_z = 60 \text{ deg}$		
$F'(150,0,40)$ $\theta_x = 0 \text{ deg}$ $\theta_y = 50 \text{ deg}$ $\theta_z = 60 \text{ deg}$		

Figure 9: Virtual images generated with the platform in both environments. Some changes in robot position and orientation have been simulated to obtain these images. (Dimensions in centimeters).

designing some algorithms to localize the robot using different kinds of environments, and incorporating these algorithms as additional options of the platform.

ACKNOWLEDGEMENTS

This work has been supported by the Spanish government through the project DPI2013-41557-P: “Navegación de Robots en Entornos Dinámicos Mediante Mapas Compactos con Información Visual de Apariencia Global” and by the Generalitat Valenciana (GVa) through the project GV/2015/031: “Creación de mapas topológicos a partir de la apariencia global de un conjunto de escenas.”

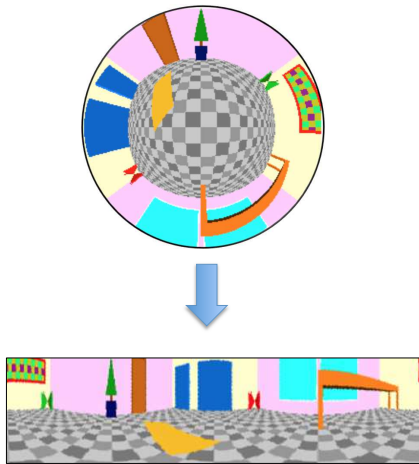


Figure 10: Sample virtual panoramic image obtained from a virtual omnidirectional image in environment 1.

REFERENCES

- Amorós, F., Payá, L., Reinoso, O., and Valiente, D. (2014). Towards relative altitude estimation in topological navigation tasks using the global appearance of visual information. In *VISAPP 2014, International Conference on Computer Vision Theory and Applications*, volume 1, pages 194–201.
- Andreasson, H. and Lilienthal, A. (2010). 6d scan registration using depth-interpolated local image features. *Robotics and Autonomous Systems*, 58(2).
- Bay, H., Tuytelaars, T., and Gool, L. (2006). Surf: Speeded up robust features. *Computer Vision at ECCV*, 3951:404–417.
- Berenguer, Y., Payá, L., Ballesta, M., and Reinoso, O. (2015). Position estimation and local mapping using omnidirectional images and global appearance descriptors. *Sensors*, 15(10):26368.
- Burbridge, C., Spacek, L., and Park, W. (2006). Omnidirectional vision simulation and robot localisation. *Proceedings of TAROS*, 2006:32–39.
- Lowe, D. (1999). Object recognition from local scale-invariant features. In *ICCV 1999, International Conference on Computer Vision*, volume 2, pages 1150–1157.
- Maohai, L., Han, W., Lining, S., and Zesu, C. (2013). Robust omnidirectional mobile robot topological navigation system using omnidirectional vision. *Engineering Applications of Artificial Intelligence*, 26(8):1942–1952.
- Mondragon, I., Olivares-Méndez, M., Campoy, P., Martínez, C., and Mejias, L. (2010). Unmanned aerial vehicles uavs attitude, height, motion estimation and control using visual systems. *Autonomous Robots*, 29:17–34.
- Nene, S. and Nayar, S. (1998). Stereo with mirrors. In *Proceedings of the 6th International Conference on Computer Vision, Bombay, India*.
- Payá, L., Amorós, F., Fernández, L., and Reinoso, O. (2014). Performance of global-appearance descriptors in map building and localization using omnidirectional vision. *Sensors*, 14(2):3033–3064.
- Payá, L., Fernández, L., Gil, L., and Reinoso, O. (2010). Map building and monte carlo localization using global appearance of omnidirectional images. *Sensors*, 10(12):11468–11497.
- Peasley, B. and Birchfield, S. (2015). Rgb point cloud alignment using lucas-kanade data association and automatic error metric selection. *IEEE Transactions on Robotics*, 31(6):1548–1554.
- Perazzi, F., Sorkine-Hornung, A., Zimmer, H., Kaufmann, P., Wang, O., Watson, S., and Gross, M. (2015). Panoramic video from unstructured camera arrays. *Computer Graphics Forum*, 34(2):57–68.
- Radon, J. (1917). Über die bestimmung von funktionen durch ihre integralwerte langs gewisser mannigfaltigkeiten. *Berichte Sachsische Akademie der Wissenschaften*, 69(1):262–277.
- Valiente, D., Gil, A., Fernández, L., and Reinoso, O. (2014). A comparison of ekf and sgd applied to a view-based slam approach with omnidirectional images. *Robotics and Autonomous Systems*, 62(2):108–119.
- Wang, X., Tang, J., Niu, J., and Zhao, X. (2016). Vision-based two-step brake detection method for vehicle collision avoidance. *Neurocomputing*, 173, Part 2:450–461.
- Winters, N., Gaspar, J., Lacey, G., and Santos-Victor, J. (2000). Omni-directional vision for robot navigation. *IEEE Workshop on Omnidirectional Vision*, pages 21–28.
- Wu, J., Zhang, H., and Guan, Y. (2014). An efficient visual loop closure detection method in a map of 20 million key locations. In *2014 IEEE International Conference on Robotics and Automation (ICRA)*, pages 861–866.
- Zivkovic, Z. and Booij, O. (2006). How did we built our hyperbolic mirror omni-directional camera practical issues and basic geometry. *Intelligent Systems Laboratory Amsterdam, University of Amsterdam, IAS technical report IAS-UVA-05-04*.